

Origin of electric field-induced magnetocrystalline anisotropy modification at Fe(001) surfaces: Mechanism of dipole formation from first principles

Kohji Nakamura,* Riki Shimabukuro, Toru Akiyama, and Tomonori Ito
Department of Physics Engineering, Mie University, Tsu, Mie 514-8507, Japan

A. J. Freeman

Department of Physics and Astronomy, Northwestern University, Evanston, Illinois 60208

(Dated: July 1, 2010)

First principles full-potential linearized augmented plane-wave studies reveal that a surface magnetocrystalline anisotropy (MCA) modification by an external electric field arises from a dipole formation mechanism. The precise calculations demonstrate that the formation of dipoles on Fe(001) surface atoms, which counteract the electric field-induced charge in the vacuum region, changes the surface states around the Fermi level in the minority-spin d bands, and yields a modification of the surface MCA. These findings greatly advance our understanding of the electric field-induced MCA modifications in itinerant ferromagnetic surfaces.

PACS numbers: 75.70.Ak, 75.30.Gw, 73.20.At, 71.20.Be

I. INTRODUCTION

Controlling and designing magnetic properties by an external electric field is a key challenge in modern magnetic physics. The electric field provides a degree of freedom for both the charge and spin of electrons that leads to a functionality in novel magnetic devices; examples are known to include magnetoelectric multiferroics and exchange bias bilayer systems.^{1,2} Surprisingly, recent experiments demonstrated that even in *itinerant thin film ferromagnets* such as thin films FePt and FePd with liquid interfaces³ and ultrathin Fe/MgO and Fe/GaAs junctions,^{4,5} the magnetocrystalline anisotropy (MCA) is modified by application of a voltage. This effect is considered currently to be attributed to a change in the number of d electrons at the surface in response to the applied electric field.³⁻⁵

Indeed, successive first principles calculations using the projector augmented wave method,⁶ pointed out an effect of the spin-dependent screening electrons at transition-metal surfaces by an electric field, which leads to a spin imbalance of the excess surface charge and may induce a modification in the surface magnetization and MCA. This prediction may, however, have an ambiguity in the precise determination of a delicate MCA energy being the order of $10^{-1}\sim 10^{-3}$ meV/atom since the calculations with a small number of k -points as done by these authors would give a large numerical error. Moreover, since the MCA originates from the spin-orbit coupling (SOC) and depends strongly on details of the d band structures,⁷ little is still known of a quantitative relation (i.e., intrinsic mechanism) between the MCA modification and the spin-dependent screening effect, which hinders the further search of new materials that exhibit stronger MCA modifications.

Most recently, an alternative mechanism for the MCA modification in an itinerant monolayer system by an electric field was proposed by means of first-principles full-

potential linearized augmented plane-wave (FLAPW) calculations.⁸ The MCA in an Fe monolayer was found to be strongly modified due to changes in the band structure introduced by the electric field, in which the p - d hybridization near the Fermi level (E_F) plays a key role. It is therefore of interest to revisit surface systems from the FLAPW calculations in order to clarify the underlying physics in the electric field-induced MCA modification.

Here, we present new results of precise FLAPW calculations for Fe(001) surfaces. Interestingly, we find that the surface MCA modification originates from the formation of dipoles on surface atoms, which counteract the electric field-induced charge in the vacuum region. Indeed, the calculated density of states (DOS) demonstrates that an enhancement/depression of the DOS in the surface states of the minority-spin d bands around E_F , accompanying with dipole formation, yields a modification of the surface MCA energy.

II. METHOD AND MODEL

The calculations were performed by the FLAPW method,⁹⁻¹¹ that treats film geometries by including fully the additional vacuum regions outside of a single slab, where the wave functions are augmented by solutions of the one-dimensional (out-of-plane) Schrödinger equation and two-dimensional plane-waves. This method has proven to be at a great advantage in accuracy for calculating surfaces/interfaces and films compared to calculations that assume a super-slab geometry (slabs separated by a vacuum region) in a bulk code. Importantly, this single slab geometry, which is non-periodic along the surface normal (z -axis), allows a natural way to include the effect of an external electric field,¹² compared to calculations that assume the super-slab geometry.^{13,14}

The external electric field potential applied along the z -axis, $v_{\text{ext}} = F_{\text{ext}}z$, is expanded into interstitial, MT sphere and vacuum regions, where F_{ext} and z are the ex-

ternal electric field and z -axis position, respectively, and the quantization axis of the spherical harmonics is set along the z -axis. Having a Hamiltonian with the added v_{ext} , self-consistent calculations are first performed in the scalar relativistic approximation (SRA), i.e., excluding the spin-orbit coupling (SOC), based on the local spin density approximation (LSDA) using the von Barth-Hedin exchange-correlation.¹⁵ LAPW functions with a cutoff of $|\mathbf{k} + \mathbf{G}| \leq 3.6$ a.u. are used, where the angular momentum expansion inside the MT sphere is truncated at $\ell = 8$ for wave functions, charge and spin density and potential.

To determine the MCA, the second variational method^{7,16} for treating the SOC is performed by using the calculated eigenvectors in the SRA, and the MCA energy, E_{MCA} , is determined by the force theorem,^{17,18} which is defined as the energy eigenvalue difference for the magnetization oriented along the in-plane $[100]$ and out-of-plane $[001]$ directions. With 7,056 special \mathbf{k} -points in the two-dimensional Brillouin zone (BZ), the E_{MCA} was found to sufficiently suppress numerical fluctuations.

In order to elucidate a mechanism in the electric field-induced MCA modification, simple systems of Fe(001) thin films are considered, by changing the number of atomic-layers from a monolayer to eleven-layers, where the in-plane lattice constant matching the fcc Ag(001) substrate ($a=5.45$ a.u.) with the c/a ratio chosen to preserve the experimental atomic volume of bcc Fe is assumed. Note that the present assumed lattice constant is very close to the bulk value (within 1 %), and we confirmed that such a small lattice variation does not much alter the results obtained.

III. RESULTS AND DISCUSSION

First, we present planar-averaged induced charge and spin densities along the z -axis, $\Delta\bar{n}(z)$ and $\Delta\bar{m}(z)$, when an electric field of 1 V/\AA is introduced. Results for a nine-layer Fe(001) film are shown in Fig. 1 (a), where arrows indicate nuclear positions of the surface atoms at S_- (negative electrode side) and S_+ (positive electrode side) sites. It is clearly seen that the induced charge appears at both sides of the slab, where the charge density is depleted at the negative electrode side while it is accumulated at the positive side, which naturally screens the external electric field so as to cause the internal electric field to vanish inside of the slab. The screening behaves in a spin-dependent way as predicted previously.⁶ Importantly, the induced charge mainly appears in vacuum regions outside of the surface atoms, and then oscillates and decays rapidly into bulk. We confirm that on the surface atom at the S_- (S_+) site, the number of electrons in the MT sphere decreases (increases) by only about 0.005 electrons compared to that in zero field, while the spin magnetic moment increases (decreases) by about $0.03 \mu_B$. However, as seen in Fig. 1 (b)-(d), a large redistribution of electrons with the combined character

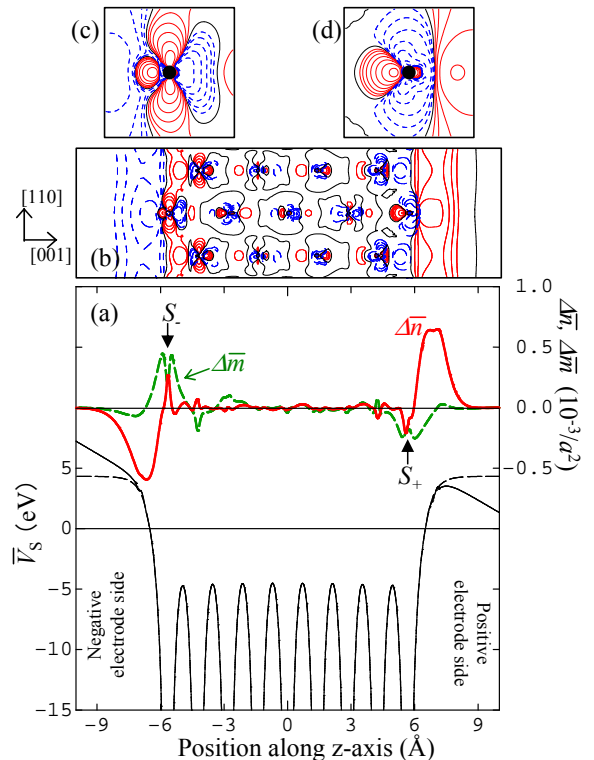


FIG. 1: (Color online) (a) Difference in calculated planar-averaged charge (thick solid line) and spin (thick dashed line) densities along the z -axis, $\Delta\bar{n}(z)$ and $\Delta\bar{m}(z)$, between the 1 V/\AA and zero field for a nine-layer film. The thin solid and dashed lines represent the calculated planar-averaged electrostatic potential, $\bar{V}_s(z)$, at 1 V/\AA and zero field, respectively, where the reference (zero) energy sets the Fermi level. Arrows indicate nuclear positions at the surfaces. (b) Contour map of charge density difference, $\Delta n(\mathbf{r})$, on a (110) plane in units of 10^{-4} electrons. Each contour line differs by a factor of 2. Solid and dashed lines indicate accumulation and depletion of electrons, respectively. Their blow-ups in (c) and (d) show details of the charge density difference on surface atoms at S_- and S_+ sites, respectively, where closed circles represent the center of surface atoms.

of p and d orbitals on the surface atoms is found to take place so as to form dipoles that counteract the electric field-induced charge in the vacuum region.

A planar-averaged electrostatic potential, $\bar{V}_s(z)$, at 1 V/\AA and zero field is also shown in Fig. 1 (a), in that the reference energy sets the Fermi level. When an electric field is introduced, the $\bar{V}_s(z)$ at the positive electrode side drops to lower energy, and the maximum value of about 3.5 eV with respect to the Fermi level is achieved at a distance of about 1.8 \AA from the surface nuclear position, which may lead to a lowering of the work function.

Now, consider the MCA. The calculated E_{MCA} at both 1 V/\AA and zero field, and their difference, ΔE_{MCA} , as a function of the film thickness are shown in Fig. 2. In zero field, E_{MCA} has positive values, indicating out-of-plane MCA. Within seven-layers, the E_{MCA} behaves like a Friedel oscillation which indicates possible size effects

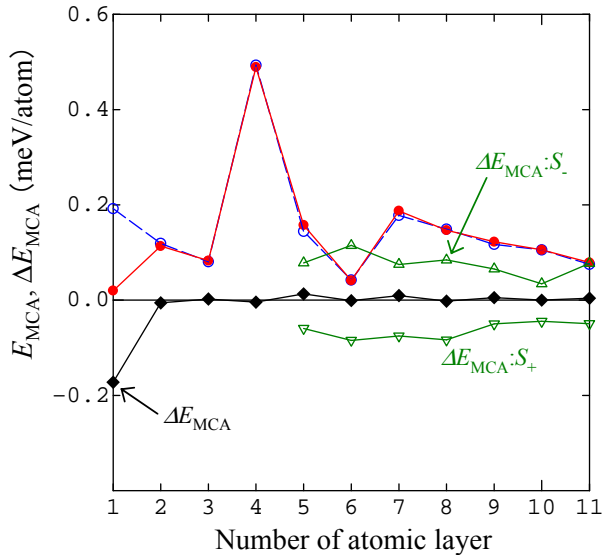


FIG. 2: (Color online) Calculated E_{MCA} at 1 V/\AA (closed circles) and zero field (open circles), and their difference, ΔE_{MCA} , (closed diamonds) as a function of the film thickness. The ΔE_{MCA} contributions from surface atoms at S_- and S_+ sites are represented by open triangles.

in such thin slabs, while when the thickness increases further it decays monotonically. When an electric field is introduced, ΔE_{MCA} in the monolayer results in about 0.2 meV/atom ,⁸ but for films thicker than the monolayer, the ΔE_{MCA} has almost zero value because of a compensation of positive and negative MCA energy contributions from both sides of the slab. Figure 2 also shows the ΔE_{MCA} contributions from the surface atoms, which are obtained by MCA calculations that artificially eliminate SOC except that on the S_- or S_+ sites, respectively. The results obtained indicate that the ΔE_{MCA} contribution from the S_- site has a positive value while that from the S_+ site, a negative value, which roughly agrees with those obtained previously.⁶

In order to further discuss the MCA modification, we calculated the partial DOS for the surface atoms and vacuum regions, which are shown in Fig. 3. As demonstrated previously,¹⁹ the minority-spin d bands of the surface atoms lie in a valley of the bonding and antibonding bulk band peaks, while the majority-spin d bands are almost fully occupied and are located from -1 to -4 eV below E_F . When the electric field is introduced, although the whole feature of the DOS does not alter much, a modification in the DOS of the minority-spin states [but not the majority-spin states] around E_F is observed, as seen in the upper figures of Fig. 3, where the modification is found to be associated with the dipole formation on the surface atoms.

Figure 4 shows the difference in the DOS of the minority-spin states, ΔN , between 1 V/\AA and zero field for the surface atoms and vacuum regions, which are further decomposed in momentum space. Two main fea-

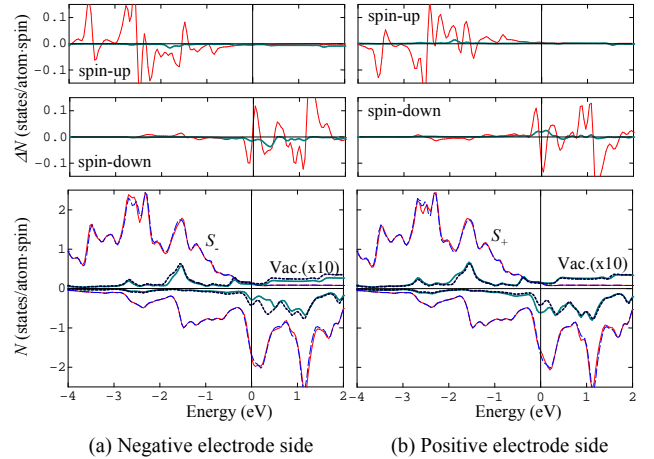


FIG. 3: (Color online) Partial density of states (DOS), N , of surface atoms at S_- and S_+ sites and vacuum regions at 1 V/\AA (solid lines) and zero field (dotted lines) for a nine-layer film. The DOS in the vacuum regions are multiplied by 10. The upper figures show the difference in the DOS, ΔN , between 1 V/\AA and zero field, where thin and thick solid lines represent results for surface atoms and vacuum regions, respectively.

tures become obvious. First, the d_{z^2} ($m = 0$) bands are strongly hybridized to the induced screening electrons in the vacuum regions through the p_z ($m = 0$) orbitals. Secondly, however, the $d_{xz,yz}$ ($m = \pm 1$) bands behave differently; the DOS around E_F for the S_- (S_+) site are enhanced (depressed). We confirmed that the surface states, having mainly $d_{xz,yz}$ orbitals, are clearly pushed up/down in energy by the electric field, as demonstrated previously for a free-standing Fe monolayer.⁸

Moreover, within the rigid band model, as seen in the upper figures of Fig. 4, the ΔE_{MCA} roughly follows the ΔN in the minority-spin $d_{xz,yz}$ bands, when the E_F is shifted. Thus, the enhancement (depression) of the DOS in the surface states of the minority-spin $d_{xz,yz}$ bands around E_F yields a positive (negative) contribution to the ΔE_{MCA} , since the SOC between occupied and unoccupied states with the same (different) m magnetic quantum number through the L_z (L_x and L_y) operator gives a positive (negative) contribution to the E_{MCA} .²⁰ In addition, the cancellation of the MCA energy between two surfaces of the slab, as presented in Fig. 2, can be explained by such a DOS enhancement (at the S_- site) and depression (at the S_+ site) around E_F in the two surfaces.

IV. SUMMARY

We investigated the effects of the external electric field on the MCA energy at the Fe(001) surfaces by means of the first principles FLAPW method, and found that the surface MCA modification originates from the dipole formation on the surface atoms, which changes the band

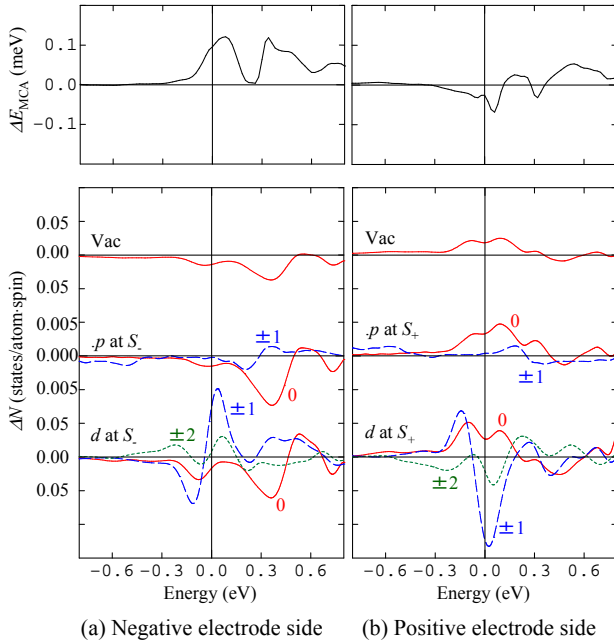


FIG. 4: (Color online) Difference in calculated density of states (DOS), ΔN , between 1 V/Å and zero field for surface atoms at S_- and S_+ sites and vacuum regions for a nine-layer film, which are further decomposed in momentum space. Only the DOS in the minority-spin states are drawn. p_0 and $p_{\pm 1}$ indicate p_z and $p_{x,y}$ states, and d_0 , $d_{\pm 1}$ and $d_{\pm 2}$ are d_{z^2} , $d_{xz,yz}$ and $d_{x^2-y^2,xy}$ states, respectively. The upper figures show the difference in the MCA energy, ΔE_{MCA} , between 1 V/Å and zero field within a rigid band model when the E_F is shifted.

structure around E_F . The large enhancement/depression in the DOS of the surface $d_{xz,yz}$ states by the electric field yields the surface MCA modification.

Acknowledgements

We thank Prof. H. J. F. Jansen for fruitful discussions on the MCA calculations. Work at Mie University was supported by a Grant-in-Aid for Scientific Research (No. 20540334), and for computations performed at ISSP, University of Tokyo. Work at Northwestern University was supported by the U.S. Department of Energy (DE-FG02-88ER 45372).

* Email address: kohji@phen.mie-u.ac.jp

- ¹ W. Eerenstein, W. Mathur, and J. F. Scott, *Nature* **442**, 759 (2006), and references therein.
- ² R. Rames and N. A. Spaldin, *Nature Mater.* **6**, 21 (2007), and references therein.
- ³ M. Weisheit, S. Fähler, A. Marty, Y. Souche, C. Poinshignon, and D. Givord, *Science* **315**, 349 (2007).
- ⁴ T. Maruyama, K. Ohta, T. Nozaki, T. Shinjo, M. Shiraishi, S. Mizukami, Y. Ando, and Y. Suzuki, *Nature Nanotech.* **4**, 158 (2009).
- ⁵ K. Ohta, T. Maruyama, T. Nozaki, M. Shiraishi, T. Shinjo, Y. Suzuki, S.-S. Ha, C.-Y. You, and W. Van Roy, *Appl. Phys. Lett.* **94**, 032501 (2009).
- ⁶ C.-G. Duan, J. P. Velev, R. F. Sabirianov, Z. Zhu, J. Chu, S. S. Jaswal, and E. Y. Tsymlal, *Phys. Rev. Lett.* **101**, 137201 (2008); note that a positive (negative) direction of an electric field is defined as an outward (inward) direction with respect to surfaces.
- ⁷ R. Wu and A. J. Freeman, *J. Magn. Magn. Mater.* **200**, 498 (1999).
- ⁸ K. Nakamura, R. Shimabukuro, Y. Fujiwara, T. Akiyama, T. Ito, and A. J. Freeman, *Phys. Rev. Lett.* **102**, 187201 (2009).
- ⁹ E. Wimmer, H. Krakauer, M. Weinert, and A. J. Freeman,

Phys. Rev. B. **24**, 864 (1981).

- ¹⁰ M. Weinert, E. Wimmer, and A. J. Freeman, *Phys. Rev. B.* **26**, 4571 (1982).
- ¹¹ K. Nakamura, T. Ito, A. J. Freeman, L. Zhong, and J. Fernandez-de-Castro, *Phys. Rev. B* **67**, 014420 (2003).
- ¹² W. Weinert, G. Schneider, R. Podloucky, and J. Redinger, *J. Phys.: Condens. matter* **21**, 084201 (2009).
- ¹³ J. Neugebauer and M. Scheffler, *Phys. Rev. B* **46**, 16067 (1992).
- ¹⁴ B. Meyer and D. Vanderbilt, *Phys. Rev. B* **63**, 205426 (2001).
- ¹⁵ U. von Barth and L. Hedin, *J. Phys. C* **5**, 1629 (1972).
- ¹⁶ C. Li, A. J. Freeman, H. J. F. Jansen, and C. L. Fu, *Phys. Rev. B* **42**, 5433 (1990).
- ¹⁷ G. H. O. Daalderop, P. J. Kelly, and M. F. H. Schuurmans, *Phys. Rev. B* **41**, 11919 (1990).
- ¹⁸ X. D. Wang, D. S. Wang, R. Q. Wu, and A. J. Freeman, *J. Magn. Magn. Mater.* **159**, 337 (1996).
- ¹⁹ S. Ohnishi, A. J. Freeman, M. Weinert, *Phys. Rev. B* **28**, 6741 (1983).
- ²⁰ D. S. Wang, R. Wu, and A. J. Freeman, *Phys. Rev. B* **47**, 14932 (1993).